UV/H$_2$O$_2$ oxidation process optimization by response surface methodology for removal of polycyclic aromatic hydrocarbons (PAHs) from water

Amirhossein Malakahmad*, Lawrence Ling Hoe Ho

Department of Civil & Environmental Engineering, Universiti Teknologi PETRONAS, Malaysia,
emails: amirhossein@utp.edu.my; amalakahmad@gmail.com (A. Malakahmad), dreamsky901120@gmail.com (L.L.H. Ho)

a b s t r a c t

Polycyclic aromatic hydrocarbons (PAHs) are persistent organic pollutants in water. They are categorized by International Agency for Research and Cancer as toxic, carcinogenic and mutagenic substances that can cause cancer and birth defect. This study was conducted to investigate the performance of ultraviolet radiation combined with hydrogen peroxide (UV/H$_2$O$_2$) for removal of PAHs from aqueous solution. The process was then optimized using response surface methodology by ranging three operating variables (hydrogen peroxide concentration, pH and reaction time) based on five-level central composite design. The significance and adequacy of the results were evaluated by analysis of variance. The model was found to be significant to give less than 0.05 probability of error and was fit with data based on insignificant of lack-of-fit test at values of 0.0005. The high R^2 and adjusted R^2 (0.8965 and 0.8771) revealed satisfactory adjustment of a quadratic model to experimental data. Application of UV/H$_2$O$_2$ process reduced PAHs concentrations in solution up to 99.4% ± 0.1%. The optimum operating condition was achieved at hydrogen peroxide concentration of 1 mM, pH of 3.5 and reaction time of 90 min. The experimental data and model prediction agreed well with error less than 3%.

Keywords: Advanced oxidation process (AOP); Carcinogenic compounds; Recalcitrant organic pollutants; Low molecular weighted PAHs; High molecular weighted PAHs

1. Introduction

The presence of persistent organic pollutants (POP) in water and wastewater is an environmental concern. Polycyclic aromatic hydrocarbons (PAHs) are one of the major classes of the POP that consists of two or more fused aromatic (benzene) rings arranged in linear, angular and cluster order and do not contain any heteroatoms and/or carry substituents [1,2]. PAHs are hydrophobic, highly stable and persistent in nature with low vapor pressure, water solubility and bio-availability [3,4]. PAHs can be classified based on their molecular weight. Low molecular weight PAHs are those with two or three aromatic rings. High molecular weight PAHs have more than three aromatic rings. The vapor pressure and water solubility decrease with increasing molecular weight of PAHs, while the resistant to chemical and biological degradation increases with increasing molecular weight of PAHs. The lower molecular weight PAHs are reported to have substantial acute toxicity to aquatic organisms, while the high molecular weight PAHs do not. However, several high molecular weight PAHs have been identified to be carcinogenic [5,6].
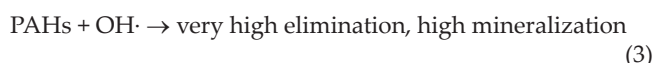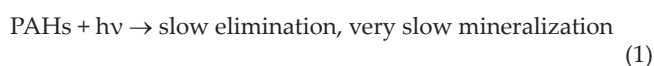
PAHs are mainly derived from anthropogenic activities that consist of petrogenic and pyrogenic sources. The accidental oil spills, discharge from routine tanker operations and municipal and urban runoff contribute to the petrogenic sources of PAHs. The pyrogenic PAHs are produced by incomplete combustion and prolysis of fossil fuels, organic materials and biomass [7,8].

Certain members of PAHs class like benzo[*a*]anthracene, chrysene, benzo[*b*]fluoranthene, benzo[*k*]fluoranthene, benzo[*a*]pyrene, dibenzo[*a,h*]anthracene, benzo[*g,h,i*]perylene and indeno[1,2,3-*c,d*]pyrene are classified as toxic, carcinogenic, mutagenic and tumorigenic to human and animals by the International Agency for Research and Cancer (IARC).
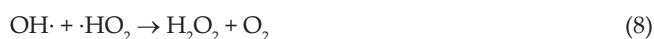
* Corresponding author.

PAHs can have detrimental effects on the affected habitats' plants and animals, resulting in uptake and bioaccumulation of toxic chemical in aquatic organisms and food chains that lead to serious health problems like cancer and birth defects in humans [9].

Among the wastewater treatment processes, advanced oxidation processes (AOPs) have received increased attention for treatment of wastewater containing recalcitrant organic pollutants. AOPs are based on the production of reactive radicals mostly hydroxyl radicals (OH·) that with an electro-chemical oxidant potential of 2.8 V and oxidation reaction of $k = 10^8 – 10^{10}$ M^{-1}s^{-1} as a strong oxidant to oxidize the organic compounds. The utilization of UV/H$_2$O$_2$ process is found to have high reaction rates due to combination of two possible degradation pathways; direct photolysis and reaction with hydroxyl radicals. A simplified reaction mechanism of the two processes is shown in Eqs. (1)–(3):

PAHs + hv → slow elimination, very slow mineralization
$$\tag{1}$$

$$H_2O_2 + h\nu \rightarrow 2OH\cdot \tag{2}$$

PAHs + OH· → very high elimination, high mineralization
$$\tag{3}$$

Hydrogen peroxide can also react with hydroxyl radicals and the intermediary products formed thereby, according to the reaction mechanism described in a simplified way by Eqs. (4)–(8) [10]:

$$H_2O_2 + OH\cdot \rightarrow \cdot HO_2 + H_2O \tag{4}$$

$$H_2O_2 + \cdot HO_2 \rightarrow OH\cdot + H_2O + O_2 \tag{5}$$

$$2OH\cdot \rightarrow H_2O_2 \tag{6}$$

$$2\cdot HO_2 \rightarrow H_2O_2 + O_2 \tag{7}$$

$$OH\cdot + \cdot HO_2 \rightarrow H_2O_2 + O_2 \tag{8}$$

The UV/H$_2$O$_2$ oxidation has been applied as treatment of water solutions containing PAHs previously [11–15]. It is noticeable that in UV/H$_2$O$_2$ process, factors such as hydrogen peroxide dose, reaction time and pH of water sample play an important role in the treatment process. Therefore, statistical optimization of these factors is an essential step that can reduce amounts of catalysts used, lessen reaction duration and decrease energy requirements without compromising the efficiency.

Among the statistical tools, response surface methodology (RSM) has been applied widely to obtain ideal process settings for the optimum performance. RSM consists of mathematical and statistical techniques used in the empirical study of the relationship between responses of interest, Y and number of input variable denoted by $x_1, x_2, \ldots x_k$ [16,17]. RSM has been used successfully to optimize the Fenton treatment of amoxicillin and cloxacilin antibiotic aqueous solution, biological augmentation of refinery wastewater, Cr(VI) reduction and removal by electrocoagulation, Fenton and electro-Fenton oxidation of biologically treated coking wastewater [18–21].

In this study, the statistical optimization of UV/H$_2$O$_2$ process was conducted for treatment of PAHs in aqueous solution using RSM.

2. Materials and methods

UV/H$_2$O$_2$ oxidation of aqueous solution that contains 16 PAHs was investigated. The treatment process was optimized using RSM for its chemical oxygen demand (COD) and PAHs removal efficiencies by manipulating three operating variables that are hydrogen peroxide concentration, pH and reaction time. The adequacy of the model was determined by analysis of variance (ANOVA) and diagnostics results. Then, final concentration of the PAHs in the aqueous solution was measured under the optimum condition to determine its removal efficiency.

2.1. Chemicals

16 PAHs (Accustandard PAH Mix, 2.0 mg/mL, Cat Z-014G-R) was purchased from AccuStandard Inc., USA. Hydrogen peroxide, H$_2$O$_2$ (30% w/w solution), and sulfuric acid, H$_2$SO$_4$ (95%–98%), were purchased from R&M Marketing, Essex, UK. Sodium hydroxide, NaOH (analytical grade, 46%–48%), dichloromethane (CH$_2$Cl$_2$) and sodium sulfate (Na$_2$SO$_4$) were purchased from Merck, Germany. H$_2$SO$_4$ and NaOH were used for pH adjustment. H$_2$O$_2$ was used for AOP, and CH$_2$Cl$_2$ and Na$_2$SO$_4$ were used for extraction of PAHs and dehydration of dichloromethane.

2.2. Samples preparation

Synthetic wastewater sample was prepared by dissolving 2 mL of PAHs standard solution mix in 1,000 mL of deionized water. The mixing was carried out to assure that PAHs were dissolved in the water completely due to their low solubility to produce more consistent PAHs concentration in the water samples. The initial COD and total organic carbon (TOC) of the prepared aqueous solution were 1,026 and 337.3 mg/L, respectively. The total PAHs concentration in the aqueous solution was 200 µg/L. The initial pH of the sample was 5.75.

2.3. Analytical methods

The individual PAHs concentration was determined by GC/MS 5975C model with Agilent 7890A GC system, direct insertion probe and pyrolizer coupled to detector – Triple Axis inert XL EI/CI MSD and mass spectrometer – Quadrupole mass analyzer. A 30 m × 250 µm × 0.25 µm film thickness HP-5MS cross-linked 5% phenylmethyl-silicone column was used with the following temperature program: 60°C for 2 min, ramp at 10°C/min to 300°C in 1 min and hold at 300°C until 29 min run time. The injector port was 360°C, and the carrier gas was helium. COD was determined according to standard methods for the examination of water and wastewater (APHA) [22]. A TOC analyzer (Model 1010; O&I Analytical) was used for determining TOC, and a pH meter with ±0.1 accuracy (HACH platinum series pH electrode model 51910, HACH Company, USA) was used for pH measurements and adjustments.

2.4. Experimental procedures

Batch experiments were conducted using a 1L Pyrex reactor filled with sample. The pH was adjusted to the required value by 1 N H_2SO_4 or 1 N NaOH. The samples were subjected to UV irradiation by an UV lamp (Spectroline model; EA-160/FE, 230 V, 0.17 A, Spectronics Corporation, New York, USA) with emitting radiation wavelength of 365 nm placed 5 cm above the reactor. The mixing was carried out by a magnetic stirrer for complete homogeneity during the reaction. Hydrogen peroxide (H_2O_2) was added according to the predefined dosages. The time at which hydrogen peroxide added to the mixture was considered as the beginning of the experiment. Aliquots were withdrawn at the time targeted. The pH of the solution was adjusted to pH > 10 to decompose H_2O_2 to oxygen and water reducing interference in COD determination. The aliquots were filtered for COD measurements. The aqueous solution was prepared by diluting the stock solution containing PAH mix. The purity of each PAH in stock solution was 97.1% and above. After subjecting of samples to UV/H_2O_2 process, they were then extracted using liquid–liquid phase extraction. PAHs were extracted by adding 100 mL of dichloromethane to 0.5 L of water sample and shaking it for 5–10 min to extract the PAHs. Then, separatory funnel was used for collection of water samples. Anhydrous sodium sulfate (Na_2SO_4) was used to absorb any remained water in the separated organic layer for drying purpose. The samples were concentrated to 5 mL by evaporation under 60°C using a rotary evaporator, and then they were analyzed using GC/MS by adding 0.5 mL acetonitrile. The total volume of each sample was 1 mL.

Preliminary analysis was divided into three sets of experiments to determine the range of operational conditions (H_2O_2 concentration, pH and reaction time). First, the experiments were carried out by varying reaction time in 15, 30, 60, 90, 120 and 150 min by dosing 3 mM of H_2O_2 and keeping the pH of the sample unadjusted at pH 5.75. Next, initial H_2O_2 concentration was varied at 0.5, 1, 3 and 5 mM to determine the range of optimum H_2O_2 concentration. Other operating variables were fixed at reaction time of 90 min and pH 5.75. Last, the experiments were carried by varying pH at 2, 4, 6 and 8 based on optimum reaction time of 90 min and H_2O_2 concentration of 1 mM.

2.5. Experimental design and mathematical modeling

In this study, Design-Expert Software (State-Ease Inc., version 6.0.7) was used for the statistical design of experiment and data analysis. The central composite design (CCD) and RSM were used to optimize the operating variables: H_2O_2 concentration (A), pH (B) and reaction time (C) for maximum COD removal efficiency (response factor) of the aqueous solution.

The range of each operating variables were established based on the predetermined range from the preliminary experiment. The coded values for H_2O_2 dosage (A), pH (B) and reaction time (C) were set at five levels: $-\alpha$ (minimum), -1, 0 (center), $+1$, and α (maximum). The design consisted of $2k$ factorial points augmented by $2k$ axial points and a center point, where k is the number of variables. Accordingly, 20 experiments were conducted with 14 experiments organized

in a factorial design (including 4 factorial points, 3 axial points and 1 center point) and the remaining 6 involving the replication of the central point to get a good estimation of experimental error. After conducting the experiments, the response (COD removal efficiency) was fitted by a second-order model in form of a quadratic polynomial equation as follows:

$$Y = \beta_0 + \sum_{i=1}^{k} \beta_i \cdot x_i + \sum_{i=1}^{k} \beta_{ii} \cdot x_i^2 + \sum_{i \leq j}^{k} \sum_{j}^{k} \beta_{ij} \cdot x_i \cdot x_j + \cdots + e \tag{9}$$

where i and j are the linear and quadratic coefficients; β is the regression coefficient; k is the number of factors studied and optimized in the experiment and e is the random error. The dependencies between the process variables, and the responses are obtained from the graphical analyses of data by ANOVA. The quality of the fitted polynomial model was expressed by the coefficient of determination R^2, and its significance was checked by the Fisher's F-test. Model terms were evaluated by the P-value with 95% confidence level. Three-dimensional plots and their respective contour plot for the COD removal efficiency based on the three operational variables were obtained. The simultaneous interaction of the factors and the response was studied from these three dimensional plot. The optimum region was identified based on the main parameter in the desirability plot.

3. Results and discussion

3.1. Preliminary analysis

3.1.1. Effect of reaction time

Initially, the experiments were carried out by varying the reaction time in the range of 15–150 min with constant dosing of 3 mM H_2O_2 concentration and keeping the pH of the samples unadjusted at pH 5.75. The results are shown in Fig. 1. At reaction time of 15, 30, 60, 90, 120 and 150 min the COD removal efficiency was 39.2%, 48.0%, 50.1%, 50.7%, 50.4% and 50.6%, respectively. It is known that H_2O_2 has maximum absorbance at λ 210–230 nm, and H_2O_2 photolysis takes place to a small extent at λ 365 nm [23]. Consequently, degradation of the PAHs when subjected to UV/H_2O_2 reaction was mainly due to the OH· radical produced by the UV/H_2O_2 reactions. The COD removal efficiency achieved equilibrium after 60 min reaction time. Previous finding indicated that the
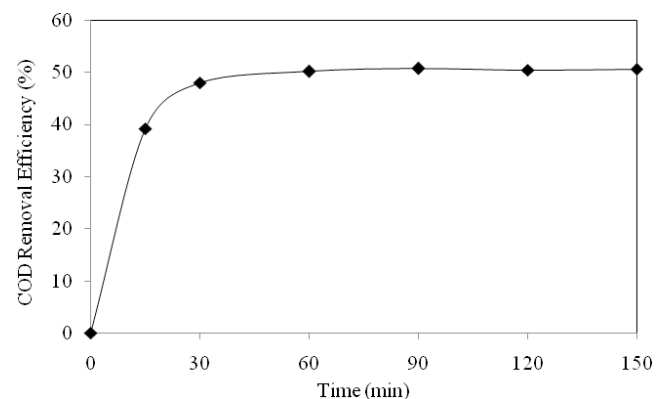

Fig. 1. Effect of time on COD removal efficiency.

UV$_{254}$ and TOC removal efficiency of creosote contaminated groundwater consisting mainly of PAHs compound also remained constant after 30 and 60 min reaction with 3 mM of H$_2$O$_2$ dosage [15]. Thus, the reaction time range of 30–90 min was used for the experimental design.

3.1.2. Effect of H$_2$O$_2$ concentration

Subsequently, initial H$_2$O$_2$ concentrations were varied in the range of 0.5–5 mM. Other operating variables were fixed at reaction time of 90 min and unadjusted pH of the sample. The results showed at concentrations of 0.5, 1, 3 and 5 mM H$_2$O$_2$, the COD removal efficiency was 43.8%, 69.2%, 50.7% and 24.8%, respectively (Fig. 2). The COD removal efficiency increased with H$_2$O$_2$ concentration from 0.5 to 1 mM and decreased with increasing H$_2$O$_2$ concentrations. The increase of hydrogen peroxide concentration generates more hydroxyl radical for the oxidation process to degrade the organic pollutants and eventually better COD removal [11]. However, in the excess of hydrogen peroxide, the hydroxyl radicals tend to undergo scavenging of OH· by H$_2$O$_2$ and formation of hydroperoxyl radical, which will lead to decrease in COD removal efficiency [13]. Therefore, the optimum range of H$_2$O$_2$ concentration used in the experimental design was 1–3 mM.

3.1.3. Effect of pH

The pH of samples was varied in the range of 2–8 while other operational variables were fixed at reaction time of 90 min and H$_2$O$_2$ concentration of 1 mM. As shown in Fig. 3, the highest COD removal efficiency was achieved at pH 2. The raise of pH from 2 to 7 increases the PAHs disappearance rate. pH > 7 results in less disappearance rate due to the oxidation inhibition [11]. Changes in pH of the reaction medium often influence the photoreaction rate, mainly due to various electron distribution in the molecule, depending on pH [24]. The photolysis of PAHs studied at different pH values indicated that the most rapid elimination of PAHs occurred at pH 2. Overall, increasing pH caused lower PAHs degradation. This is probably due to changes in the extinction coefficient of PAHs with respect to pH. The results were in a good agreement with the other reported researches [11–13]. Thus, the pH range of 2–5 was selected for the experimental design.

3.2. Statistical analysis

RSM was applied to optimize the removal efficiency based on three operating variables (H$_2$O$_2$ concentration, pH and reaction time) of UV/H$_2$O$_2$ oxidation. The low and high ranges of the operating variables were chosen from the preliminary experiments. Table 1 shows the range and level of operating variables. The CCD was used to design the experiments. The outcome indicated 20 sets of experimental condition to be tested. Table 2 shows the experimental conditions and results of CCD.

The fitting of data to various models (linear, two factorial, quadratic and cubic) and their subsequent ANOVA presented that the COD removal efficiency of the samples was mostly suitably described by a quadratic model. The multiple regression coefficients of a second-order polynomial model were summarized in Table 3. The significance of each variable was
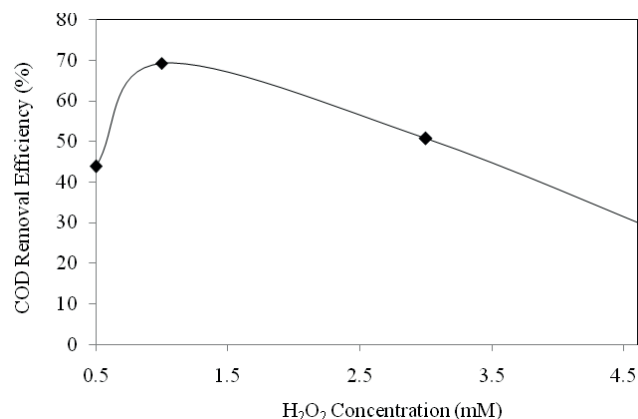

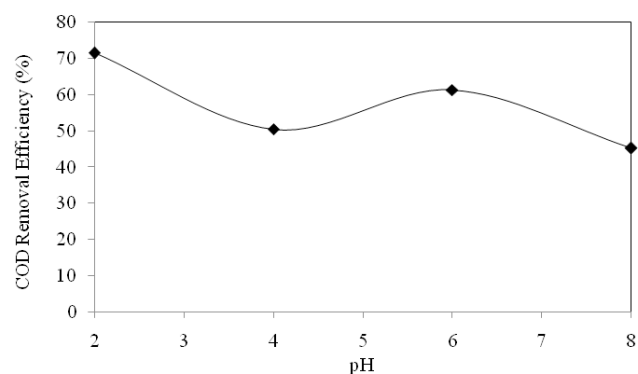Fig. 2. Effect of H$_2$O$_2$ concentration on COD removal efficiency.

Fig. 3. Effect of pH on COD removal efficiency.

Table 1
The range and level of operating variables

Variable	Code	Range and levels				
		$-\alpha$	-1	0	1	α
H$_2$O$_2$ concentration, mM	A	0.32	1	2	3	3.68
pH	B	0.98	1	3.5	5	6.02
Reaction time, min	C	0.55	30	60	90	110.45

determined by F-value and p-value. Corresponding p-values suggest that, among the test variables investigated in this study, C, B^2 and C^2 are significant model term. Other model terms, with probability values more than 0.05, are insignificant. Thus, to simplify model, the insignificant terms (A, B, A^2, AB, AC and AB) were eliminated. The effect of terms on the response was indicated by the normalized coefficients and the normalized coefficients are presented in Fig. 4. As it can be seen in the figure, the first-order effect of reaction time (C), second-order effect of pH (B^2) and second-order effect of reaction time (C^2) have the main effects on COD removal.

Regression equation, the empirical model in terms of coded factors for the response, is shown in Eq. (10) before the elimination of the insignificant model. Regression equation after elimination of the insignificant model terms is presented in Eq. (11):

Table 2
Experimental condition and results of central composite design

Run	H_2O_2 concentration (mM) (A)	pH (B)	Reaction time (min) (C)	COD removal efficiency (%)
1	1 (–1)	2 (–1)	30 (–1)	47.95
2	3 (1)	2 (–1)	30 (–1)	48.68
3	1 (–1)	5 (1)	30 (–1)	61.05
4	3 (1)	5 (1)	30 (–1)	54.32
5	1 (–1)	2 (–1)	90 (1)	76.15
6	3 (1)	2 (–1)	90 (1)	76.28
7	1 (–1)	5 (1)	90 (1)	78.04
8	3 (1)	5 (1)	90 (1)	72.94
9	0.32 (–1.682)	3.5 (0)	60 (0)	71.51
10	3.68 (1.682)	3.5 (0)	60 (0)	77.73
11	2 (0)	0.98 (–1.682)	60 (0)	70.52
12	2 (0)	6.02 (1.682)	60 (0)	58.22
13	2 (0)	3.5 (0)	0.55 (–1.682)	43.37
14	2 (0)	3.5 (0)	110.45 (1.682)	88.95
15	2 (0)	3.5 (0)	60 (0)	73.42
16	2 (0)	3.5 (0)	60 (0)	74.59
17	2 (0)	3.5 (0)	60 (0)	73.29
18	2 (0)	3.5 (0)	60 (0)	73.49
19	2 (0)	3.5 (0)	60 (0)	75.47
20	2 (0)	3.5 (0)	60 (0)	74.37

Table 3
Estimated regression coefficients and corresponding ANOVA results from data of central composite design experiments before elimination of insignificant model terms

|	Coefficient estimate	Sum of squares (SS)	Degree of freedom (DF)	Mean square (MS)	F-value	P-value	
Quadratic model	74.22	2,539.97	9	282.22	13.61	0.0002	Significant
A	–0.037	0.019	1	0.019	9.155E-004	0.9765	Not significant
B	–0.25	0.84	1	0.84	0.041	0.8441	Not significant
C	12.31	2,068.28	1	2,068.28	99.71	<0.0001	Significant
A^2	–0.58	4.84	1	4.84	0.23	0.6393	Not significant
B^2	–4.2	254.66	1	254.66	12.28	0.0057	Significant
C^2	–3.57	183.75	1	183.75	8.86	0.0139	Significant
AB	–1.59	20.13	1	20.13	0.97	0.3478	Not significant
AC	0.13	0.13	1	0.13	6.393E-003	0.9378	Not significant
BC	–2.52	50.95	1	50.95	2.46	0.1481	Not significant
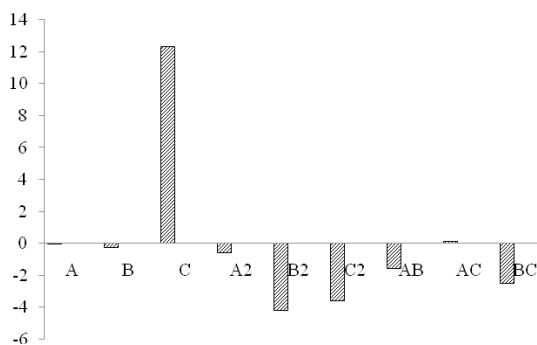
Fig. 4. Normalized coefficient of the model.

$$Y = 74.22 - 0.037\ A - 0.25\ B + 12.31\ C - 0.58\ A^2 - 4.15\ B^2 - 3.57\ C^2 - 1.59\ AB + 0.13\ AC - 2.52\ BC \tag{10}$$

$$Y = 74.22 + 12.31\ C - 4.15\ B^2 - 3.57\ C^2 \tag{11}$$

The adequacy and significance of results were analyzed and viewed in ANOVA as shown in Table 4.

The quadratic model with P-value (<0.0001) was significant to give less than 0.05 of probability of error. The F-test for lack of fit (PLOF) describes the variation of data around the fitted model. If the model does not fit well, then PLOF will be significant. The larger P-value for PLOF (>0.05)

showed the F statistics was insignificant; indicate significant model correlation between variables and process responses. In this study, the PLOF value was 0.0005, which indicate that the model was significant. The R^2 coefficient indicates the ratio of sum of squares due to regression (SSR) to total sum of squares (SST). It gives the proportion of the total variation in the response by the model. A high R^2 value, close to 1, is desirable as reasonable agreement with adjusted R^2 [25]. R^2 should be at least 0.80 for a good fit of a model [26]. The analysis gives 0.8965 and 0.8771 R^2 and adjusted R^2 values, respectively. These values are greater than 0.8 and indicate a satisfactory adjustment of the quadratic model to the experimental data has been achieved. Adequate precision (AP) compares the range of predicted values at the design points to the average prediction error. In this case, the AP value of 21.956 (greater than 4) indicates adequate model discrimination, and it can be used to navigate design space defined by CCD [27]. The coefficient of variance (CV) as the ratio of estimate standard error to the mean value of the observed response defines the reproducibility of the model. A model can be considered reproducible if its CV is not greater than 10%. Low value of the coefficient of variation designates a very high degree of precision and good deal of reliability of the experimental values [20]. In this study, the CV is about 6.15%, which indicates the model is reproducible. The predicted residual error sum of squares (PRESS) is the ordinary residual weighted according to the diagonal elements of the hat matrix [28]. In this study, the difference between the ordinary residual (3.68) and PRESS residual (579.98) is large that specify a point where the model fits the data well.

To verify residue analysis of the response surface design and to ensure that the statistical assumptions fit the analysis data, the fit of data was interpreted by diagnostics results such as normal probability plot of residuals, outlier plot and predicted vs. actual values plot. Fig. 5(a) shows the normal probability of the residuals to verify whether the standard deviation between the actual and predicted response values follows a normal distribution [29]. The residues fall near to a straight line; thus, there is no clear indication of non-normality of experimental results. The plot of residual vs. predicted responses is shown in Fig. 5(b). All points of experimental runs were scattered randomly within the constant range of residuals across the graph that within the horizontal lines at the point of ±1.75 with only two points lies above the +1.75 horizontal line. This implies that the proposed models are adequate and that the constant variance assumption was confirmed. Fig. 5(c) shows the predicted vs.
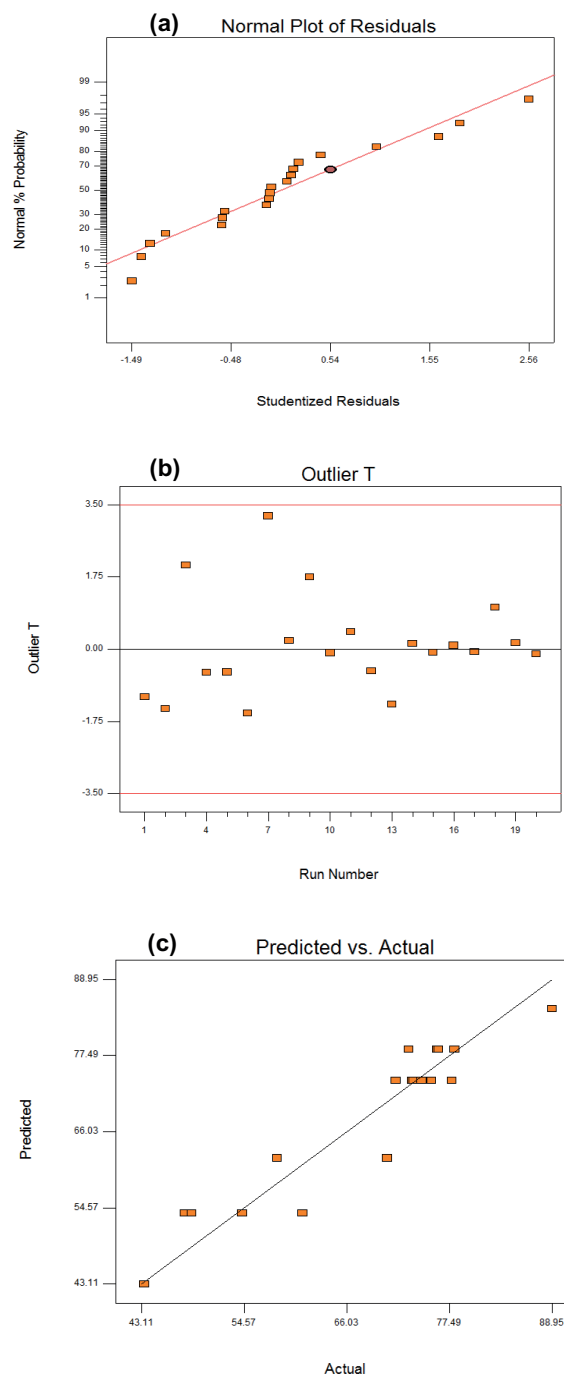

Fig. 5. Residue analysis of the response surface design verification: (a) normal probability plot of residue, (b) plot of residue vs. predicted response, and (c) predicted vs. actual values plot for COD removal efficiency augmentation.

Table 4
ANOVA results for response parameter

Response	COD
Significant model terms	C, B^2 and C^2
P	<0.0001
PLOF	0.0005
R^2	0.8965
Adj. R^2	0.8771
AP	21.956
S.D.	4.22
CV	6.15
PRESS	579.98

Note: P: probability of error; PLOF: probability of lack of fit; R^2: determination coefficient; Adj. R^2: adjusted determination coefficient; AP: adequate precision; S.D.: standard deviation; CV: coefficient of variance; and PRESS: predicted residual error sum of squares.

actual values plot for COD removal efficiency augmentation. All the responses from experimental results fitted well within an acceptable variance range when compared with the predicted values from respective empirical models.

3.3. Process optimization

In the numerical optimization, the desired goal was chosen for each factor and response from the menu. The possible goals are: maximize, minimize, target, within range, none (for responses only) and set to an exact value (factors only). The goals are combined into an overall desirability function. Desirability is an objective function that ranges from zero outside of the limits to one at the goal [28]. The optimization was done by setting goals for each response as shown in Table 5 to generate optimal condition as shown in Table 6.

Based on the solutions generated by the Design Expert Software shown in Fig. 6, the optimum condition (H_2O_2 concentration of 1 mM, pH of 3.5 and reaction time of 90 min) predicted by RSM for the maximum COD removal efficiency (82.5%). Desirability value of 0.927 was adopted for the verification experiment. It should be noted that the increase in reaction time from 90 to 112.58 min predicts the increment of COD removal efficiency of 1.98% with higher desirability value of 0.950. But, this solution does not offer a significant improvement in COD removal efficiency while the reaction time is prolonged to another 20 min.

3.4. Model verification and efficiency of UV/H_2O_2 oxidation in reduction of PAHs in aqueous solution

Photodegradation of PAHs in an aqueous solution is a complex mechanism involving ubiquitous oxygen. Intermediates competing for light and oxygen with target molecules can be involved in the reaction too [30]. In order to validate the optimum point generated by central composition design, three experiment runs were carried out under the optimum conditions (H_2O_2 concentration of 1 mM, pH of 3.5 and reaction time of 90 min) to verify the results predicted by the model. The COD removal efficiency value obtained from the experiment was 79.8%, which is in acceptable agreement with estimated value by the model (82.5%) with less than 3% error. After validation of the model, an aqueous solution containing premeasured concentration of PAHs was treated based on optimized condition achieved in previous step. Average concentration of standard solution was 19.91 µg/L. The standard solution contained 16 PAHs. The concentrations of PAHs in the sample before treatment and each PAH removal efficiency under the optimized condition are shown in Table 7. Physical and chemical characteristics of PAHs vary with molecular weight. For instance, PAHs resistance to oxidation, reduction and vaporization increases with increasing molecular weight, whereas the aqueous solubility of these compounds decreases. Results indicate that the average removal percentage of the seven potentially carcinogenic PAHs was more than 86%. BaA and BaP, which are considered as most probably carcinogenic PAHs to human [31], had very noticeable eliminations (close to 90%) by application of UV/H_2O_2 oxidation. The achieved efficiencies in removal of phenanthrene, fluoranthene and pyrene are higher than those achieved by Nkansah et al. [32] using light-weight expanded clay aggregate and those findings reported by Krupadam et al. [33] on adsorbing PAHs on molecularly imprinted polymers.

PAH's degradation can be accomplished in different pathways. It could be either through radical cation or participation of oxygen: via a singlet oxygen ($^1O_2$) and via a

Table 5
The goal set for each constraint

Constraint	Goal	Lower limit	Upper limit
H_2O_2 concentration	Minimize	1	3
pH	In range	2	5
Reaction time	In range	30	90/150
COD removal efficiency	Maximize	43.47	88.95

Table 6
Numerical optimization for central composite design

Solution No.	H_2O_2 concentration (A)	pH (B)	Reaction time (C)	COD removal efficiency	Desirability
1	1.00	3.50	112.58	84.52	0.950
2	1.00	3.50	112.45	84.52	0.950
3	1.00	3.50	112.32	84.52	0.950
4	1.00	3.50	112.77	84.52	0.950
5	1.00	3.54	112.63	84.52	0.948
6	1.00	3.83	109.76	84.30	0.948
7	1.00	3.08	114.86	84.17	0.946
8	1.00	3.50	90.00	82.54	0.927
9	1.00	3.51	89.28	82.54	0.927
10	1.00	3.57	89.23	82.53	0.927
11	1.00	3.49	90.00	82.54	0.921
12	1.00	2.90	90.00	81.89	0.919
13	1.00	3.79	85.22	81.45	0.914
14	1.00	4.94	90.00	78.74	0.881

Table 7
The PAHs removal efficiency and concentrations of PAHs in the sample before and after treatment

No.	Name	Structure	Toxicity level in water[a]	Concentration in solution before subjecting to UV/H_2O_2 (µg/L)	Removal efficiency (%)
1	Acenaphthene (Ace)		3	20.01	96.9 ± 0.6
2	Acenaphthylene (Acy)		NC	19.85	98.3 ± 0.1
3	Anthracene (Ant)		3	19.93	99.4 ± 0.1
4	Benzo[*a*]anthracene (BaA)		2B	20.02	89.5 ± 0.5
5	Benzo[*a*]pyrene (BaP)		1	19.98	89.4 ± 0.5
6	Benzo[*b*]fluoranthene (BbF)		2B	20.00	84.7 ± 0.5
7	Benzo[*g,h,i*]perylene (BghiP)		3	19.69	84.5 ± 0.3
8	Benzo[*k*]fluoranthene (Bkf)		2B	20.01	88.0 ± 0.1
9	Chrysene (Chr)		2B	19.80	85.5 ± 0.1
10	Dibenz[*a,h*]anthracene (DahA)		2A	19.68	79.7 ± 0.1
11	Fluoranthene (Flu)		3	20.01	89.5 ± 0.5
12	Fluorene (Fluo)		3	19.84	95.0 ± 0.5
13	Indeno(1,2,3-*cd*)pyrene (IcdP)		2B	20.01	87.6 ± 1.0
14	Naphthalene (Nap)		3	19.92	96.0 ± 0.5
15	Phenanthrene (Phe)		3	19.91	95.0 ± 0.5
16	Pyrene (Pyr)		3	19.84	95.7 ± 0.3

[a]Based on IARC (International Agency for Research on Cancer) classification of carcinogenicity: 1: carcinogen to human; 2A: probably carcinogen to human; 2B: possibly carcinogen to human; 3: not classifiable as to its carcinogenicity to human; and NC: not classified.

hydroxyl radical made in some reactions from a superoxide anion [30]. Photon resulted from UV radiation, absorbed by the PAH molecules and caused their excitation. Those excited molecules can dissipate energy in aqueous solution again in several ways, mostly photophysical processes like internal intersystem crossing, fluorescence, conversion, and by energy transfer to other molecules. An excited PAH molecule can also undergo chemical changes, for instance, proton or electron transfer.

PAHs are known as good sensitizers for singlet oxygen formation [34]. Sensitizers are substances other than catalysts, which enable the starting of catalytic reactions. Oxygen in the ground triplet state needs above 94 kJ mol^{-1} to transform into a very reactive singlet state [35]. An excited PAH molecule can deliver this energy to oxygen.

Electron transfer with the formation of a radical cation could cause degradation of PAHs too. In that path, a radical cation reacts with water or hydroxide ion to give the alcohol
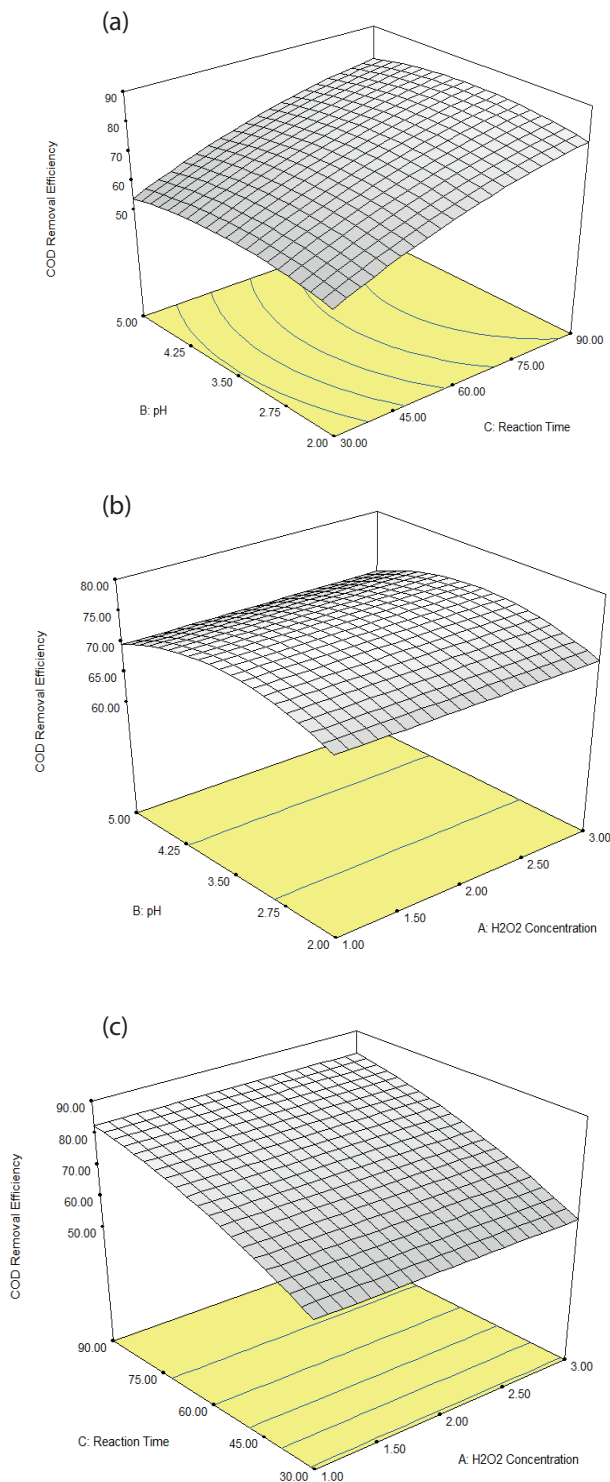
(a)

(b)

(c)

Fig. 6. The three-dimensional response surface plots in COD removal efficiency.

radical, which then either reacts with oxygen to yield quinone (organic compounds derived from PAHs by conversion of an even number of –CH= groups into –C(=O)– groups) as a major stable product or polymerizes in deoxygenated solutions.

The total PAHs removal efficiency of low molecular weight PAHs (Ace, Acy, Ant, Fluo, Nap and Phe) was more than 96%. The high removal of low molecular weight PAHs is an important achievement due to their acute toxicity to aquatic organisms. The results are comparable with those achieved by Turek et al. [36] for removal of 16 PAHs from aqueous solution using titanium catalyst and Włodarczyk-Makuła et al. [37] for removal PAHs from coking wastewater during photodegradation process. The degradation of low molecular PAHs was noticeably faster compared with those achieved via biodegradation. Daugulis and McCracken [38] reported complete biodegradation of naphthalene, phenanthrene and fluoranthene using *Sphingomonas aromaticivorans* and *Sphingomonas paucimobilis* after 16 h.

4. Conclusions

The UV/H_2O_2 oxidation was found to be effective for the treatment of PAHs in aqueous solution. The process optimization by RSM based on CCD was significant in utilization of less catalyst and reducing the process duration. Under the optimum operating condition (H_2O_2 concentration of 1 mM, pH of 3.5 and reaction time of 90 min), the suggested COD removal efficiency by the model was 82.5%. The experimental removal efficiency and the model prediction were in satisfactory agreement with less than 3% error. The average PAHs removal efficiencies were 96.0% and 87.4% for low and high molecular weight PAHs, respectively. The outcomes of this work indicate that the UV/H_2O_2 oxidation process is reliable method for removal of PAHs from aqueous solution. Application of UV/H_2O_2 oxidation process is beneficial for those industries that have PAHs in their wastewater.

Acknowledgment

Symbols

i	—	Linear coefficient
j	—	Quadratic coefficients
β	—	Regression coefficient
k	—	Number of factor studied and optimized in the experiment
e	—	Random error
P	—	Probability of error
PLOF	—	Probability of lack of fit
R^2	—	Determination coefficient
Adj. R^2	—	Adjusted determination coefficient
AP	—	Adequate precision
SD	—	Standard deviation
CV	—	Coefficient of variance
PRESS	—	Predicted residual error sum of squares

References

[1] P. Garrigues, H. Budzinski, M.P. Manitz, S.A. Wise, Pyrolytic and petrogenic inputs in recent sediments - a definitive signature through phenanthrene and chrysene compound distribution, Polycycl. Aromat. Compd., 7 (1995) 275–284.

[2] M.P. Zakaria, K.H. Geik, W.Y. Lee, R. Hayet, Landfill leach-ate as a source of polycyclic aromatic hydrocarbons (PAHs) to Malaysian waters, Coast. Mar. Sci., 29 (2005) 116–123.

[3] S.E. Allan, B.W. Smith, K.A. Anderson, Impact of the deepwater horizon oil spill on bioavailable polycyclic aromatic hydrocarbons in Gulf of Mexico coastal waters, Environ. Sci. Technol., 46 (2012) 2033–2039.

[4] H. Gupta, B. Gupta, Adsorption of polycyclic aromatic hydrocarbons on banana peel activated carbon, Desal. Wat. Treat., 57 (2016) 9498–9509.

[5] C. Sauret, M. Tedetti, C. Guigue, C. Dumas, R. Lami, M. Pujo-Pay, P. Conan, M. Goutx, J.F. Ghiglione, Influence of PAHs among other coastal environmental variables on total and PAH-degrading bacterial communities, Environ. Sci. Pollut. Res., 23 (2016) 4242–4256.

[6] N.K. Nagpal, Ambient Water Quality Criteria for Polycyclic Aromatic Hydrocarbons (PAHs), Ministry of Environment, Lands and Parks, Province of British Columbia, Water Quality Branch, Water Management Division, 1993.

[7] M.P. Zakaria, A.A. Mahat, Distribution of polycyclic aromatic hydrocarbon (PAHs) in sediments in the Langat Estuary, Coast. Mar. Sci., 30 (2006) 387–395.

[8] M.P. Zakaria, H. Takada, S. Tsutsumi, K. Ohno, J. Yamada, E. Kouno, H. Kumata, Distribution of polycyclic aromatic hydrocarbons (PAHs) in rivers and estuaries in Malaysia: a widespread input of petrogenic PAHs, Environ. Sci. Technol., 36 (2002) 1907–1918.

[9] S.K. Samanta, O.V. Singh, R.K. Jain, Polycyclic aromatic hydrocarbons: environmental pollution and bioremediation, Trends Biotechnol., 20 (2002) 243–248.

[10] O.M. Alfano, R.J. Brandi, A.E. Cassano, Degradation kinetics of 2,4-D in water employing hydrogen peroxide and UV radiation, Chem. Eng. J., 82 (2001) 209–218.

[11] F.J. Beltrán, G. Ovejero, J. Rivas, Oxidation of polynuclear aromatic hydrocarbons in water. 3. UV radiation combined with hydrogen peroxide, Ind. Eng. Chem. Res., 35 (1996) 883–890.

[12] F.J. Rivas, F.J. Beltrán, B. Acedo, Chemical and photochemical degradation of acenaphthylene. Intermediate identification, J. Hazard. Mater., 75 (2000) 89–98.

[13] Y.J. An, E.R. Carraway, PAH degradation by UV/H_2O_2 in perfluorinated surfactant solutions, Water Res., 36 (2002) 309–314.

[14] V.J. Pereira, H.S. Weinberg, K.G. Linden, P.C. Singer, UV degradation kinetics and modeling of pharmaceutical compounds in laboratory grade and surface water via direct and indirect photolysis at 254 nm, Environ. Sci. Technol., 41 (2007) 1682–1688.

[15] S. Vilhunen, M. Vilve, M. Vepsäläinen, M. Sillanpää, Removal of organic matter from a variety of water matrices by UV photolysis and UV/H_2O_2 method, J. Hazard. Mater., 179 (2010) 776–782.

[16] K.D. Lin, J.J. Peterson, Statistical Inference for Response Surface Optimaization, Response Surface Methodology and Related Topics, London, 2009.

[17] A.I. Khuri, S. Mukhopadhyay, Response surface methodology, WIREs Comput. Stat., 2 (2010) 128–149.

[18] T. Ölmez, The optimization of Cr(VI) reduction and removal by electrocoagulation using response surface methodology, J. Hazard. Mater., 162 (2009) 1371–1378.

[19] X. Zhu, J. Tian, R. Liu, L. Chen, Optimization of Fenton and electro-Fenton oxidation of biologically treated coking wastewater using response surface methodology, Sep. Purif. Technol., 81 (2011) 444–450.

[20] S. Ishak, A. Malakahmad, Optimization of Fenton process for refinery wastewater biodegradability augmentation, Korean J. Chem. Eng., 30 (2013) 1083–1090.

[21] A.C. Affam, M. Chaudhuri, S.R.M. Kutty, K. Muda, UV Fenton and sequencing batch reactor treatment of chlorpyrifos, cypermethrin and chlorothalonil pesticide wastewater, Int. Biodeterior. Biodegrad., 93 (2014) 195–201.

[22] APHA, Standard Methods for Examination of Water and Wastewater, 21st ed., Wahsington, D.C., USA, 2005.

[23] J.J. Pignatello, D. Liu, P. Huston, Evidence for an additional oxidant in the photo assisted Fenton reaction, Environ. Sci. Technol., 33 (1999) 1832–1839.

[24] T. Mill, W.R. Mabey, B.Y. Lan, A. Baraze, Photolysis of polycyclic aromatic hydrocarbons in water, Chemosphere, 10 (1981) 1281–1290.

[25] S.D. Ashrafi, S. Nasseri, M. Alimohammadi, A.H. Mahvi, M.A. Faramarzi, Optimization of the enzymatic elimination of flumequine by laccase-mediated system using response surface methodology, Desal. Wat. Treat., 57 (2016) 14478–14487.

[26] A. Gallina, A. Martowicz, T. Uhl, Robustness analysis of a car windscreen using response surface techniques, Finite Elem. Anal. Des., 47 (2011) 46–54.

[27] M.Y. Noordin, V.C. Venkatesh, S. Sharif, S. Elting, A. Abdullah, Application of response surface methodology in describing the performance of coated carbide tools when turning AISI 1045 steel, J. Mater. Process. Technol., 145 (2004) 46–58.

[28] A. Malakahmad, S.Y. Chuan, Application of response surface methodology to optimize coagulation–flocculation treatment of anaerobically digested palm oil mill effluent using alum, Desal. Wat. Treat., 51 (2013) 6729–6735.

[29] M.A. Masigol, A. Moheb, A. Mehrabani-Zeinabad, Comprehensive study on interactive effects of operational parameters by using response surface method for sodium sulfate removal from magnesium stearate aqueous slurry via electrodialysis process, Desal. Wat. Treat., 57 (2016) 14145–14157.

[30] J.S. Miller, D. Olejnik, Photolysis of polycyclic aromatic hydrocarbons in water, Water Res., 35 (2001) 233–243.

[31] International Agency for Research on Cancer (IARC), Polynuclear Aromatic Compounds, Part 1, Chemical, Environmental and Experimental Data, IARC Monographs on the Evaluation of the Carcinogenic Risk of Chemicals in Humans, 1983.

[32] M.A. Nkansah, A.A. Christy, T. Barth, G.W. Francis, The use of lightweight expanded clay aggregate (LECA) as sorbent for PAHs removal from water, J. Hazard. Mater., 217–218 (2012) 360–365.

[33] R.J. Krupadam, M.S. Khan, S.R. Wate, Removal of probable human carcinogenic polycyclic aromatic hydrocarbons from contaminated water using molecularly imprinted polymer, Water Res., 44 (2010) 681–688.

[34] A.M. Braun, M.-Th. Maurette, E. Oliveros, Photochemical Technology, J. Wiley & Sons. New York 1991.

[35] S.L. Murov, I. Carmichael, G. L. Hug, Handbook of Photochemistry, Marcel Dekker, 2nd ed., New York 1993.

[36] A. Turek, M. Włodarczyk-Makuła, W.M. Bajdur, Effect of catalytic oxidation for removal of PAHs from aqueous solution, Desal. Wat. Treat., 57 (2016) 1286–1296.

[37] M. Włodarczyk-Makuła, E. Wiśniowska, A. Turek, A. Obstój, Removal of PAHs from coking wastewater during photodegradation process, Desal. Wat. Treat., 57 (2016)1262–1272.

[38] A.J. Daugulis, C.M. McCracken, Microbial degradation of high and low molecular weight polyaromatic hydrocarbons in a two-phase partitioning bioreactor by two strains of *Sphingomonas sp.*, Biotechnol. Lett., 25 (2003) 1441–1444.